agronomy

IMPACT FACTOR 3.7

CITESCORE 5.2

Article

Research and Experiment on Soybean Plant Identification Based on Laser Ranging Sensor

Shenghao Ye, Xinyu Xue, Zhu Sun, Yang Xu, Tao Sun, Jinwen Ye and Yongkui Jin

MDPI

https://doi.org/10.3390/agronomy13112757 *agronomy*

Article

Research and Experiment on Soybean Plant Identification Based on Laser Ranging Sensor

Shenghao Ye [1,2], Xinyu Xue [1], Zhu Sun [1], Yang Xu [1], Tao Sun [1], Jinwen Ye [1,2] and Yongkui Jin [1,*]

[1] Nanjing Institute of Agricultural Mechanization, Ministry of Agriculture and Rural Affairs, Nanjing 210014, China; 82101215529@caas.cn (S.Y.); xuexinyu@caas.cn (X.X.); sunzhu@caas.cn (Z.S.); xuyang01@caas.cn (Y.X.); suntao@caas.cn (T.S.); 82101215528@caas.cn (J.Y.)

[2] Graduate School of Chinese Academy of Agricultural Sciences, Beijing 100081, China

[*] Correspondence: jinyongkui@caas.cn

Abstract: When endeavoring to study the complex growth conditions of soybean plants under natural conditions, a problem arises due to the similar appearances of both soybean plants and weeds. To address this issue, a soybean plant recognition model based on a laser ranging sensor is proposed. To demonstrate the applicability of the soybean plant recognition model, experiments are conducted using ultrasonic sensors and laser ranging sensors to analyze the diameter, height, and spacing conditions in the model. A test environment is built, and during the pre-test, the laser range sensor detects objects with diameters of 3 mm and 5 mm with two and three measurement points, respectively, at a speed of 0.2 m/s. At a speed of 0.3 m/s, there is one measurement point for objects with 3 mm diameter and two measurement points for objects with 5 mm diameter. At 0.4 m/s, there are also one and two measurement points for objects with diameters of 3 mm and 5 mm, respectively. These results demonstrate that the laser range sensor can more accurately recognize the diameter conditions of soybean plants and weeds and can distinguish between the diameters of soybean plants and weeds. Subsequently, the recognition rate of the model is evaluated by observing whether the weeding mechanism can synchronize seedling avoidance after the soybean plant passes through the sensor. The recognition rates of the optimized model at speeds of 0.2 m/s, 0.3 m/s, and 0.4 m/s are 100%, 98.75%, and 93.75%, respectively. Upon comprehensive analysis, the soybean plant recognition model is determined to achieve a recognition rate of 98.75% at a speed of 0.3 m/s, which is considered a moderate speed, and demonstrates more stable recognition of plant diameters. The test further verifies the reliability and effectiveness of the method for distinguishing between soybean plants and weeds. The research results can serve as a reference for recognizing soybean plants based on the use of laser ranging sensors.

Keywords: soybean; laser ranging sensor; soybean plant recognition model; recognition rate

Citation: Ye, S.; Xue, X.; Sun, Z.; Xu, Y.; Sun, T.; Ye, J.; Jin, Y. Research and Experiment on Soybean Plant Identification Based on Laser Ranging Sensor. *Agronomy* **2023**, *13*, 2757. https://doi.org/10.3390/agronomy13112757

Academic Editor: Mario Cunha

Received: 21 September 2023
Revised: 23 October 2023
Accepted: 24 October 2023
Published: 1 November 2023

1. Introduction

In recent years, with the development of agricultural science and technology, the improvement of soybean production has become one of the world's top agricultural development priorities. However, the growth environment of soybeans is complex, and the growth of weeds has an impact on soybeans, as they compete with soybean plants in the early growth phase for light, water, and nutrients. If left unchecked, weeds will seriously jeopardize soybean quality and yield [1]. Mechanical weed control is a common alternative to chemical weed control [2,3]. Mechanical weed control aims to maximize weed control and effectively minimize seedling injury, so accurate detection of target objects and improved weed control mechanisms or weed control modes are critical [4,5].

Historically, distinguishing between soybeans and weeds was primarily a process involving manual identification, which was inefficient, involved a heavy workload, and represented a severe waste of human resources. Various methods have been used for weed identification in past decades, from RTK (Real Time Kinematic) and GPS to spectroscopy [6–8].

The principle of these methods lies in detecting the target crop using these methods. If the target crop is identified as a soybean plant, it is preserved. If it is not a soybean plant, it is treated as a weed and subjected to weed control operations. In contrast, deep learning technology-based detection methods and LiDAR recognition are increasingly being used in agriculture [9–11].

With machine vision, a camera captures and processes an image using various techniques [12]. This enables the system to learn the features and patterns of the image, which can help with identifying soybeans and weeds. The method involves comparing and classifying features such as the color, shape, and texture of the image [13]. Hu Lian et al. [14] presented a crop recognition and localization technique that utilizes machine vision. They used Otsu image segmentation and morphological operations to identify crops by analyzing their row–column pixel accumulation curves, curve standard deviation, and sine wave curve fitting. The study found that the method achieved a 100% correct recognition rate for lettuce seedlings and 95.8% for cotton seedlings. However, the method may still encounter errors in locating plant leaves and roots when the weed density is high. Zhang Jingyu et al. [15] collected and produced a dataset of 8000 images to establish a corn seedling and weed detection model based on deep learning technology. Then, they selected the YOLOv4 detection network and, after 20,000 iterations of learning, obtained the seedling and weed recognition model. This model's highest accuracy, recall, F1 value, and mAP are 96.07%, 96.59%, 96.27%, and 95.17%, respectively, and the model performs well. However, the preliminary preparation work is cumbersome, and there is a high demand for optimal lighting conditions. Liu Yachao et al. [16] wrote a specific image recognition algorithm for the real-time acquisition of complex growth environments in the field, based on OpenCV image processing software, and completed the identification of plants and weeds by writing an image-processing program using the C programming language. However, in plant recognition, the recognition rate is higher in the case of good light intensity, and the recognition rate is only 65.5% in the case of low light intensity, during which, plants cannot be distinguished well from weeds. Although deep learning has the advantages of high accuracy and adaptivity for recognizing plants and weeds, image recognition is sensitive to environmental conditions such as light and shadows. The accuracy of recognition is often affected by the complexity of the image background, the similarity of the crop and weed morphology, and environmental factors [17]. Deep learning requires a large amount of data and computational resources as well as complex training and testing [18]. LiDAR obtains the shape and contour information of the target object by scanning to realize the recognition of weeds [19]. David Reiser et al. [20] mounted LiDAR on the front of a small four-wheeled robot that collected time-stamped data as it traveled across the field and fused it with data from a total station to generate a 3D point cloud. This 3D point cloud is used to detect the position of individual plants with high accuracy and can detect all plants (100% detection rate) with an accuracy of 2.7–3.0 cm at a plant spacing of 13 cm. However, this approach cannot be performed in real-time, as the data needs to be collected first, and it is difficult to generalize the application because of its high cost. LiDAR identification can be used in all-weather conditions and demonstrates high accuracy, but it has higher requirements for processing data and field environment parameters.

In addition, Li Sensen et al. [21] replaced the visual recognition method with a mechanical sensing approach for distinguishing corn and weeds which uses a flexible shaft as the signal input for the mechanical sensing because the flexible shaft does not deform when it collides with weeds, as the weeds are too soft, while it does deform when it collides with corn stalks. When the deformation of the flexible shaft reaches a certain angle, the object detected is regarded as a corn plant, which is, in turn, transformed into a recognition signal. Although this approach is less costly, it has more limitations in practical application; it requires higher requirements for the appearance characteristics of plants and weeds, and at the same time, does not take into account the various morphologies of plants and weeds in different growth periods or variations in leaf distribution, and is not well suited to complex field environments [22]. Chen Xueshen et al. [23] proposed a tactile perception method based on the physiological height and mechanical differences between rice and weeds during the weeding period, through mechanical analysis, established a mechanical model of the contact role of the perception beam and the rice plant, combined with the bending strength of the rice plant, and designed a perception beam for the positioning of the rice plant. However, the positioning of the plant in this way is easily affected by the traveling speed of the machine and the planting spacing and density.

To solve the above problems, this study proposes a method based on a sensor that can measure distance and can thus determine the measured object's diameter, height, and agronomic planting spacing requirements to establish the corresponding recognition model. Ultrasonic sensors are more adaptable to the environment [24]. Laser-ranging sensors are characterized by high accuracy, high speed, and high stability, can avoid the influence of light, shadow, and other environmental factors, are low cost, and are more effective in use [25]. When the mechanical weeding device encounters soybeans, it can successfully perform seedling avoidance action. For the different morphological characteristics of soybean plants and weeds, ultrasonic and laser ranging sensors were used for testing according to the soybean plant identification model.

2. Materials and Methods

2.1. Test Materials and Data Collection Principles

2.1.1. Test Materials

The soybean recognition model test is carried out on a test platform, shown in Figure 1a, and consists of a conveyor belt, a fixed frame, a sensing device, and a weeding mechanism. Figure 2 shows a schematic diagram of the conveyor belt, which is 3670 mm long and 660 mm wide, and the weeding mechanism is fixed in the position of the fixed frame in Figure 1b. The adjustment range of the conveyor belt running speed is between 0.1 m/s and 2 m/s, with an adjustment scale of 0.05 m/s. When the sensor detects a target, it passes the distance data to the PLC (Programmable Logic Controller), which determines whether or not the target is a soybean plant by using the soybean recognition model. According to the running speed of the conveyor belt and the horizontal distance between the sensor and the weeding mechanism, the PLC sends commands to the servo motor, controlling the weeding mechanism to synchronize the seedling avoidance action.

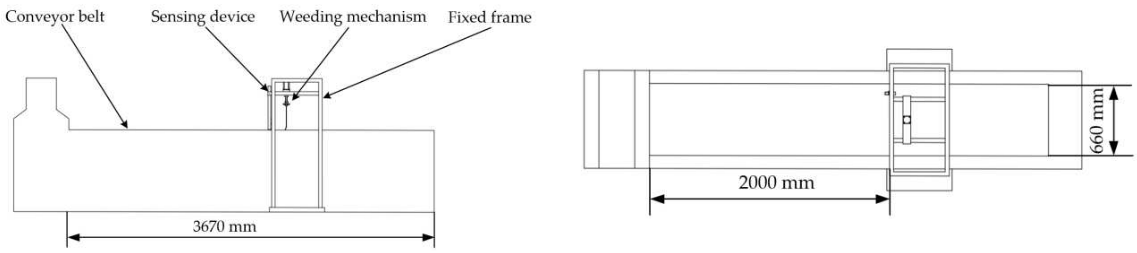

(**a**) (**b**)

Figure 1. Schematic diagram of test platform structure: (**a**) composition diagram of test platform; (**b**) fixed frame positioning diagram.

Figure 2. Conveyor belt.

The test material consisted of ultrasonic sensors (UT 12-370-A-IL4, manufactured by SensoPart, Shanghai, China.), laser ranging sensors (BL-200NMZ, manufactured by BOJKE, Shenzhen, China), a PLC, and a laptop.

The sensing device consists of two laser ranging sensors, one positioned above and the other below, as shown in Figure 3. The lower laser ranging sensor is located 70 mm above the soil surface, with a distance of 100 mm between the upper and lower photometer laser beams. This installation aims to accurately determine the position of the soybean plant, ensuring synchronization between the weeding mechanism and seedling avoidance actions. The BL-200NMZ model laser ranging sensors can be set within a range of 120 mm–280 mm, and the soybean planting row spacing is 300 mm, so the two sensors can be placed to the side of the soybean plant at a distance of about 200 mm to prevent contact of the soybean leaf with the sensor, thus avoiding interference. The laser ranging sensor emits a visible laser beam with a diameter of 0.5 mm, and the sensor feeds back out of range when no object is detected; when an object is detected within the range, the sensor feeds back the specific data distance.

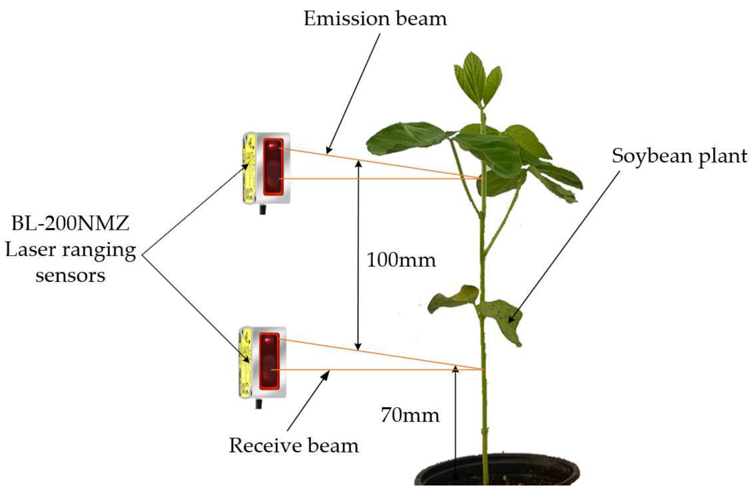

Figure 3. Two Laser-ranging sensors detect the height localization of soybean plants.

SIMATIC S7-200SMART (manufactured by SIEMENS AG, headquartered in Munich, Germany) is the selected PLC, the CPU model is the ST30 (manufactured by SIEMENS AG, Munich, Germany), and the analog input module with S7-200SMART selected is the EM AE04 (manufactured by SIEMENS AG, Munich, Germany), which has four analog input ports. The performance of the S7-200SMART is very stable, it can meet many different work requirements, it is simple to use, easy to learn and operate, and can work well with other tools.

The weeding mechanism is shown in Figure 4, which is mainly composed of a servo motor (TSDA-C21B, manufactured by Vacsin, Shenzhen, China), frame, spindle, guide slider, flange disk, connecting rod, fixed rod, comb plate, and profiled elastic combs. The servo controller sends pulses to make the servo motor rotate, the servo motor drives the flange disk to rotate through the spindle, and the comb plate is connected with the connecting rod and the fixed rod. When the flange disc drives the connecting rod, the two comb plates will expand outward under the action of the fixed rod and the guide rail. Thus, the switching back-and-forth between the weed-avoiding state and the seedling-avoiding state is facilitated, and the seedling-avoidance and weeding operations are performed. The elastic comb teeth penetrate the soil surface to a certain depth, and during the movement, the comb teeth will brush the weed rhizomes out of the soil or cut and pull the weed rhizomes to achieve the effect of weeding.

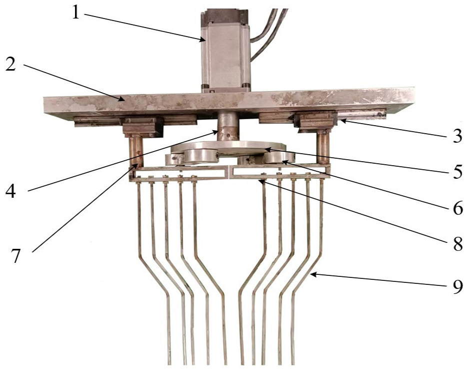

Figure 4. Schematic diagram of weeding mechanism: (1) Motor; (2) Frame; (3) Guide rail slider; (4) Spindle; (5) Flange disc; (6) Connecting rod; (7) Fixed rod; (8) Comb plate; (9) Profiling elastic comb teeth.

The installation positions of the sensing device and the weeding mechanism are shown in Figure 5. Two laser ranging sensors are placed, with the beam of the lower sensor 70 mm above the ground and the distance between the beams of the upper and lower sensors set at 100 mm. The horizontal distance between the sensing device and the weeding mechanism is 100 mm to allow the sensors to detect objects. By including a soybean plant recognition model in the PLC programming, the PLC can differentiate soybean plants and send control commands to the servo motor, enabling the weeding mechanism to perform synchronized seedling avoidance actions. Two sensors are connected on the same square tube, which can be adjusted up and down. The bottom of the square tube is positioned 50 mm above the surface of the conveyor belt.

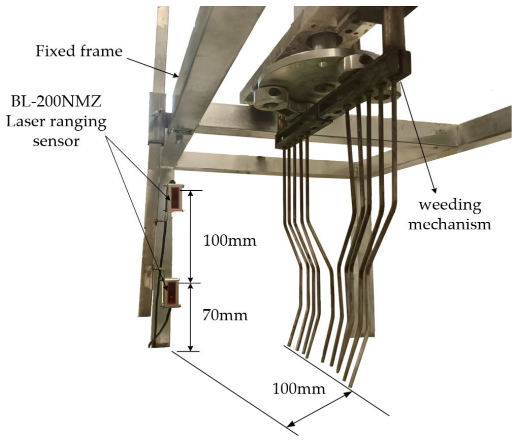

Figure 5. Installation position diagram of sensing device and weeding mechanism.

The laser ranging sensor has a response time of 1.5 ms, with a sampling frequency of 4ms (without averaging). The combined response time for data collection and soybean plant recognition is approximately 5 ms. Compared to image recognition, the response time for real-time data collection is shorter, and the operation is simpler.

The general flow chart of the soybean recognition model is shown in Figure 6. The sensor detects the target object and passes the signal to the control system. The soybean recognition model is programmed into the PLC control system, and the model determines whether the target object is a soybean plant. If so, the PLC will send an action command to the servo drive, the servo drive will send pulses to the servo motor to synchronize the weeding mechanism with the seedling avoidance action, and will then wait for the next target object to meet the model.

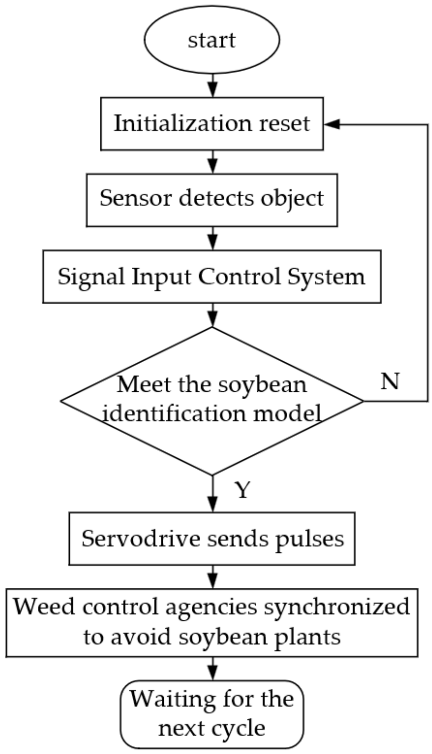

Figure 6. Overall flowchart of the soybean plant identification model.

2.1.2. Data Acquisition and Control Principle

This paper's instruments for collecting data are ultrasonic and laser range sensors. The sensors input the distance data into the PLC through analog current, and the program in the PLC is set to record the distance data fed back from the sensors every 10 ms. The schematic diagram is shown in Figure 7, and the data logs are exported once for every set of data tested. The PLC will collect the distance data from the soybean plant recognition model to distinguish whether the measured object is a soybean plant. If it is a soybean plant, the PLC, according to the encoder speed wheel feedback of the current speed, the horizontal distance between the sensing device, and the weeding mechanism, calculates the time for the soybean plant to reach the weeding mechanism. At the same time, the PLC sends control instructions to the servo drive so that when the soybean plant reaches the weeding mechanism, the weeding mechanism can synchronize the seedling avoidance.

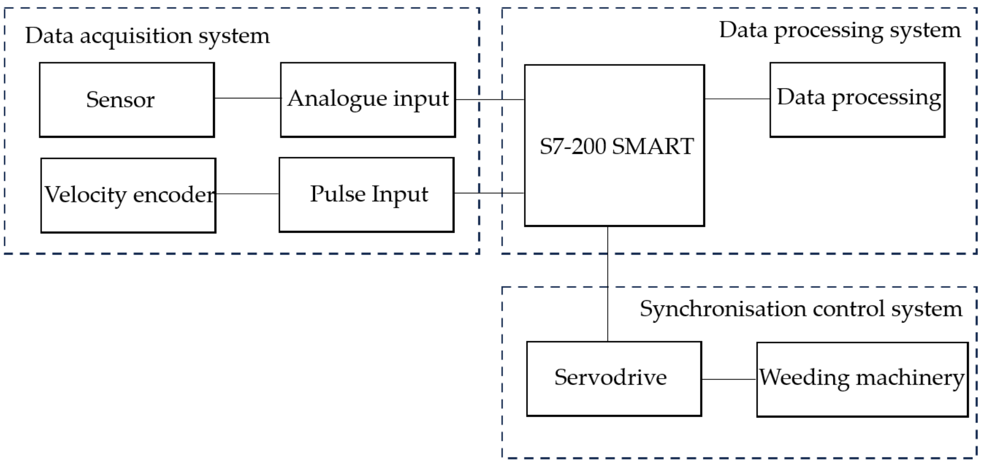

Figure 7. Schematic diagram of data acquisition and control.

According to the control preset requirements function, the control system should include one digital input signal for the speed wheel encoder A-phase clock and B-phase clock; two analog input signals, respectively, for the upper and lower two different sensors; and no digital output signals. One of the input point variable address assignment tables is shown in Table 1.

Table 1. Input variable address assignment table.

Input	Name
I0.0	Tacho Wheel Encoder Phase A Clock
I0.1	Tacho Wheel Encoder Phase B Clock
0+	Lower sensor positive terminal
0−	Lower sensor negative terminal
1+	Upper sensor positive terminal
1−	Upper sensor negative terminal

2.2. Sensor Calibration and Hardware Wiring

2.2.1. Sensor Calibration

The laser range and ultrasonic sensors transmit the distance data to the S7-200SMART PLC through the analog current output. Therefore, it is necessary to calibrate the laser range sensor and the ultrasonic sensor before the test, record the current analog value corresponding to each 1 cm in the actual sensor, and determine the relationship between the analog signal and the actual distance through the algorithm and analysis.

In the calibration process, 24V DC voltage was added to the laser range sensor and ultrasonic sensor, respectively, and the laser range sensor was calibrated from 120–280 mm and measured every 10 mm; the ultrasonic sensor was calibrated from 30–400 mm and measured every 10 mm. Each data set was repeated five times to remove the outliers generated by poor operation during measurement and the average value was taken.

The fitting algorithm from MATLAB (2016 a) was used to give the appropriate function of the laser range sensor data, as shown in Figure 8. From Figure 8, the correspondence function between the analog signal and the distance parameter is obtained:

$$y = 0.0007239x + 8.005 \tag{1}$$

where, y represents the analog signal and x represents the distance.

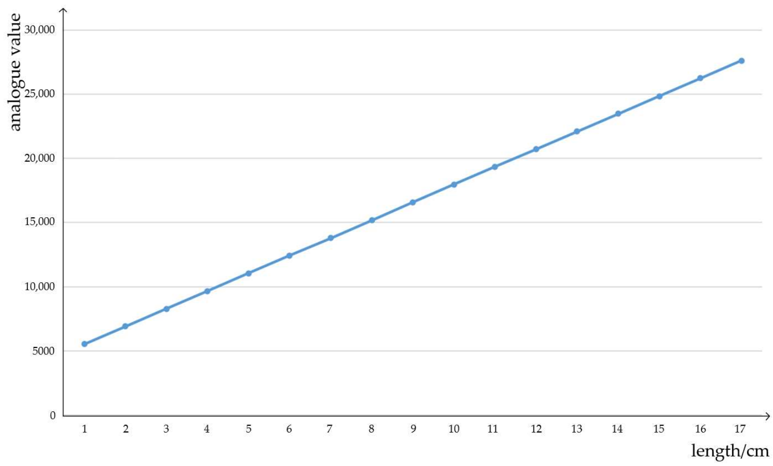

Figure 8. Diagram of the relationship between the simulated signal of the laser sensor and actual distance.

Similarly, the ultrasonic sensor data fitting function is also given, as shown in Figure 9. From Figure 9, the correspondence function between the analog signal and the distance parameter is given as:

$$y = 0.00156x - 3.648 \tag{2}$$

where, y represents the analog signal and x represents the distance.

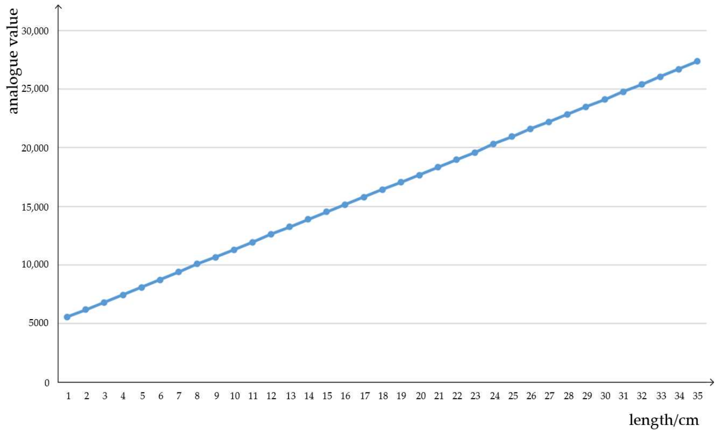

Figure 9. Diagram of the relationship between the simulated signal of the ultrasonic sensor and the actual distance.

2.2.2. Hardware Connection

This control system has many different devices, and the voltage used is mainly 24V DC. The list of electrical hardware devices is shown in Table 2.

Table 2. List of major electrical hardware.

Serial Number	Name of Equipment	Number
1	S7-200 SMART PLC	1
2	laser ranging sensor	2
3	ultrasonic sensor	1
4	servodrive	1
5	velocity wheel encoder	1

The electrical hardware power supply diagram is shown in Figure 10. The switching power supply provides 220V AC to 24V DC to the PLC, sensors, servo drives, velocity wheel encoder, and other hardware power supply to ensure the stable operation of the hardware of each module in the system.

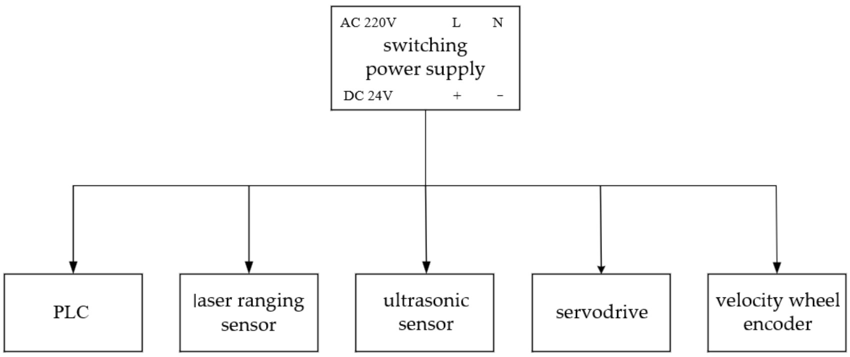

Figure 10. Electrical hardware power supply diagram.

The laser ranging sensors detect distance information through analog output lines (+) and (−). However, if the analog voltage output time is too long, it can cause unstable output data. Therefore, analog current output is used instead.

Their analog output lines (+) are connected to the 0+ input port and 1+ input port of the PLC analog input module EM AE04 to connect the two ranging sensors. The STEP 7-MicroWIN SMART software V2.7 provided by SIMATIC S7-200 SMART is used to program the algorithm that relates the analog quantity to the distance achieved by calibrating the laser ranging sensors.

The PLC is connected to the self-contained RS485 communication interface via an RS485 conversion line at one end, while the other is connected to the RS485 network port of the servo drive. The servo drive is connected to the motor power line and motor coding line at one end, and the other end is connected to the servomotor. The servomotor is then fixedly attached to the weed-removal mechanism through the shaft.

2.3. Modeling for Soybean Plant Identification

Through the pre-analysis of soybean and weed morphology, as shown in Figure 11, it is understood that the best time to weed soybean plants is the three-leaf stage. At this time, the diameter of the soybean plant is 4–5 mm, while the weeds around the soybean plant are generally short, and the stalk's diameter is below 3 mm. In addition to the difference in diameter, there is also a clear height difference. The three-leaf stage of the soybean has a height average of about 250 mm, while the height of the average weed is 70–100 mm, some may exceed 150 mm. Coupled with the spacing requirements of agronomic cultivation of soybean plants, a soybean plant spacing of 100 mm satisfies the three major identification rules: diameter, height, and spacing.

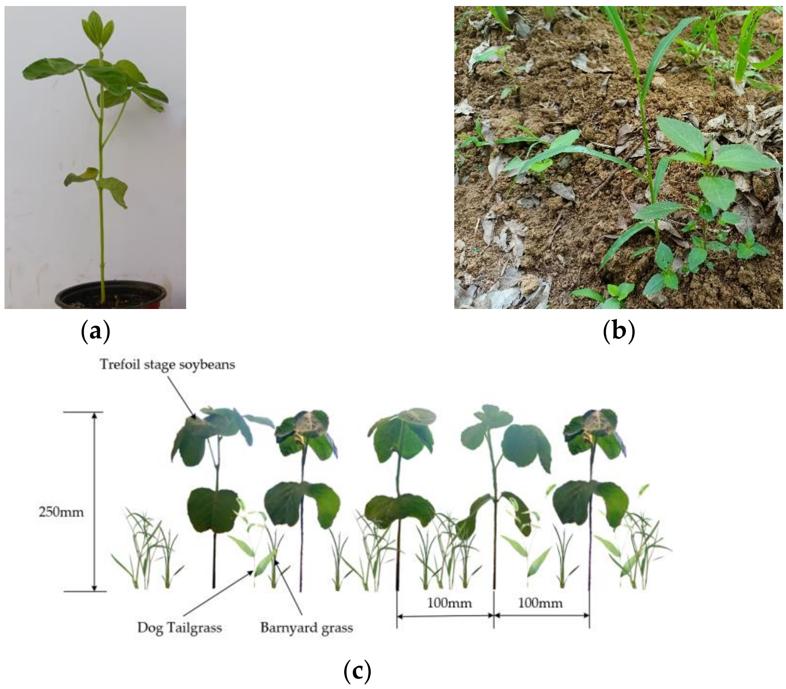

Figure 11. Morphological characteristics of soybeans and weeds: (**a**) trefoil stage soybeans; (**b**) rank grass; (**c**) the height and spacing of soybean during the trefoil stage, as well as its distribution among surrounding weeds.

Here, the preprocessing model is established. From the point set, data can be distinguished from the different diameters of the object, but there will be stray point interference, resulting in invalid points that are not within the range. The range of the laser range sensor is d_{min}–d_{max}. Thus, the algorithmic processing is carried out as follows:

$$f(x) = \begin{cases} d_{min} \le d \le d_{max} \text{and} |d_0 - d| \le n, & x = 1 \\ d \le d_{min}, & x = 0 \\ d \ge d_{max}, & x = 0 \end{cases} \quad (3)$$

where, d represents the distance between the laser range sensor and the object to be measured; d_0 represents the distance between the next laser range sensor and the object to be measured; d_{min} represents the minimum range of the laser range sensor; d_{max} represents the maximum range of the laser range sensor; and n is the point set data, representing the difference between the points of the previous point and the points of the next one.

To differentiate between the height of soybean plants and weeds, two laser ranging sensors are needed, both upper and lower. Since soybean plants are taproot systems with well-developed main roots and vertical stalks, the condition of height can only be satisfied when both upper and lower photometers recognize the object.

Thus, the soybean plant recognition model is defined as follows:

The measurement schematic is shown in Figure 12 for the diameter condition:

$$D = vt \tag{4}$$

$$f(c) = \begin{cases} d_{min} \leq x_1 \leq d_{max}, & c = 1 \\ x_1 \leq d_{min}, & c = 0 \\ x_1 \geq d_{max}, & c = 0 \end{cases} \tag{5}$$

$$f(c) = \begin{cases} d_{min} \leq x_2 \leq d_{max} \text{and} |x_2 - x_1| \leq n, & c = 2 \\ x_2 \leq d_{min}, & c = 0 \\ x_2 \geq d_{max}, & c = 0 \end{cases} \tag{6}$$

$$c = \sum_{i=1}^{n} x_n, d_{min} \leq x_n \leq d_{max} \text{and} |x_{n+1} - x_n| \leq n \tag{7}$$

where, D represents the diameter of the object to be measured; v represents the running speed; t represents the time from the beginning to the end of the detection of the object to be measured; x_1 represents the distance data recorded in the current 10 ms; x_2 represents the distance data recorded in the next 10 ms; d_{min} represents the minimum range of the laser ranging sensor; d_{max} represents the maximum range of the laser ranging sensor; n is the point set data, representing the difference between the points of the previous point and the points of the next one; and c represents the recorded value.

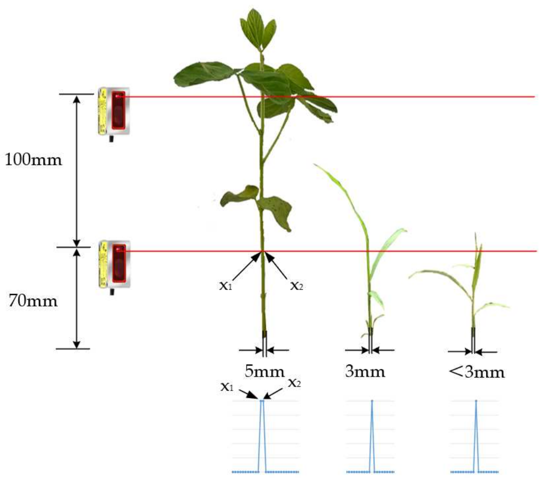

Figure 12. Diameter measurement and judgment schematic diagram.

The measurement schematic is shown in Figure 13 for the height condition:

$$f(x_h) = \begin{cases} |x_{hs} - x_{hx}|, & x_h \leq m \\ d_{min} \leq d_{hs} \leq d_{max} \\ d_{min} \leq d_{hx} \leq d_{max} \end{cases} \tag{8}$$

where, d_{hs} represents the distance data between the upper laser ranging sensor and the object being measured; x_{hs} represents the position of the upper laser ranging sensor when it detects the object; d_{hx} represents the distance data between the lower laser ranging sensor and the object being measured; x_{hx} represents the position of the lower laser ranging sensor when it detects the object; x_h represents the difference between the two sensors detecting the position of the object in the horizontal direction; and m represents the difference between the two horizontal positions.

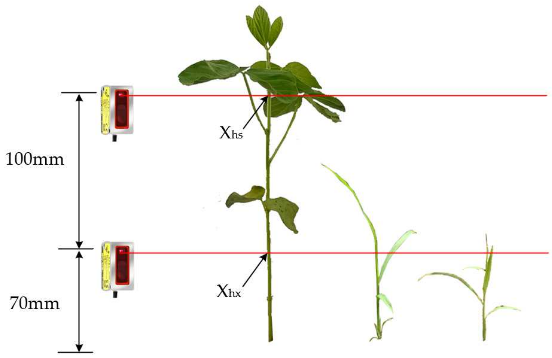

Figure 13. Height measurement and judgment schematic diagram.

The measurement schematic is shown in Figure 14 for the spacing condition:

$$f(x_l) = \left| x_{lq} - x_{lh} \right|, \quad a \leq x_l \leq b \tag{9}$$

where, x_{lq} represents the position of the previous soybean plant; x_{lh} represents the position of the subsequent soybean plant; x_l represents the spacing between the previous and subsequent soybean plants; a represents the minimum threshold for the spacing between the previous and subsequent soybean plants; and b represents the maximum threshold for the spacing between the previous and subsequent soybean plants.

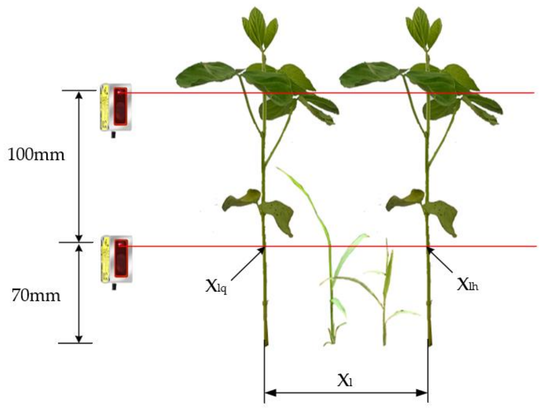

Figure 14. Distance measurement and judgment schematic diagram.

When the PLC reads the distance data from the laser distance sensor within the range, and at the same time, the difference between two consecutively recorded distance data points are not more significant than n, n is generally taken as 9, and the record is 1.

If the distance data read in the next 10 ms is within the range, a value of 1 will be added to the record, raising the value to 2. If it is not within the range, the record value will be cleared, and the system will wait for the next instance to check if the condition can be satisfied. The record value will be 1 again. When the record value is 0 or 1, no object is detected on the surface, or weed(s) may be detected. The diameter condition will be satisfied when the record value is greater than or equal to 2.

For the judgment of the height condition, the threshold m is set to 9 mm due to the straight stem of the soybean plant. When the upper sensor detects distance data, the lower sensor is within the threshold range and records a value greater than or equal to 2; or when the lower sensor records a value greater than or equal to 2, the upper sensor detects distance data within the threshold range. Both of these cases satisfy the height condition.

According to the requirements of agricultural planting, the spacing between soybean plants is 100 mm. After judging the first plant as a soybean plant, the spacing condition will be added, and to avoid any errors regarding the spacing of soybean plants during planting, the threshold value is set to 30 mm. At this time, a is 7, and b is 13.

At the same time, the height difference between soybean plants and weeds is huge, and weeds are generally short at the three-leaf stage of soybean. To reduce the possibility of misjudgment in cases which the diameters of soybean plants are around 3 mm, when the diameter record value is 1, and the height and spacing simultaneously meet the requirements, the subject is also determined to be a soybean plant.

In addition, considering the complexity of the field environment, if the lower laser ranging sensor detects a leaf when the upper sensor also detects an object, as shown in Figure 15, it is necessary to reprogram. For example, at a speed of 0.3 m/s, the lower sensor (c = 2) will meet the diameter condition. When this occurs, a restriction c less than 4 should be added. At this point, the soybean plant recognition model will no longer mistake soybean leaves for stems. In general, the lowest height of the leaves of a three-leaf stage soybean plant is 90 mm, and the height of the laser ranging sensor detection is 70 mm. Basically, the leaves will not interfere with the detection.

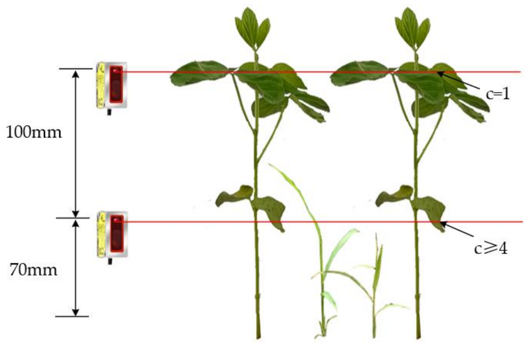

Figure 15. Soybean leaf shading judgment schematic diagram.

3. Test Procedure and Data Analysis

3.1. Pre-Laboratory

This test was conducted in the laboratory of the Nanjing Institute of Agricultural Mechanization, Ministry of Agriculture and Rural Affairs, where pre-processing tests were conducted to verify the suitability of ultrasonic sensors and laser ranging sensors to detect the diameter of objects.

The ultrasonic sensors were tested by placing the soybean plants on a conveyor belt and allowing the belt to run at a speed of 0.3 m/s. The ultrasonic sensors were placed perpendicular to the conveyor belt and, in terms of height, were placed in the upper-middle and lower-middle portions of the soybean plant, respectively. When the ultrasonic sensors detected the soybean plants passing by, the distance data were transmitted to the PLC through an analog current. A graph of the distance data derived from the PLC is shown in Figure 16, in which the horizontal axis of the coordinates represents the time. The vertical axis represents the distance between the sensors and the object to be measured.

The tests found that with ultrasonic sensors at the same speed, the distance image of the detection of the lower middle of the soybean plant and the detection of the upper middle of the soybean plant was inconsistent. The reason is that the ultrasonic sensors detect a wide range and are not sensitive to small differences, leading to the ultrasonic sensors detecting the position of the soybean leaves. The exported distance data would be a line segment with no undulation, thus, the soybean and weeds could not be distinguished well. Observed from the image of the data with obvious undulations, the number of points of each undulation is not the same, and there is no regularity to prove the size of its diameter.

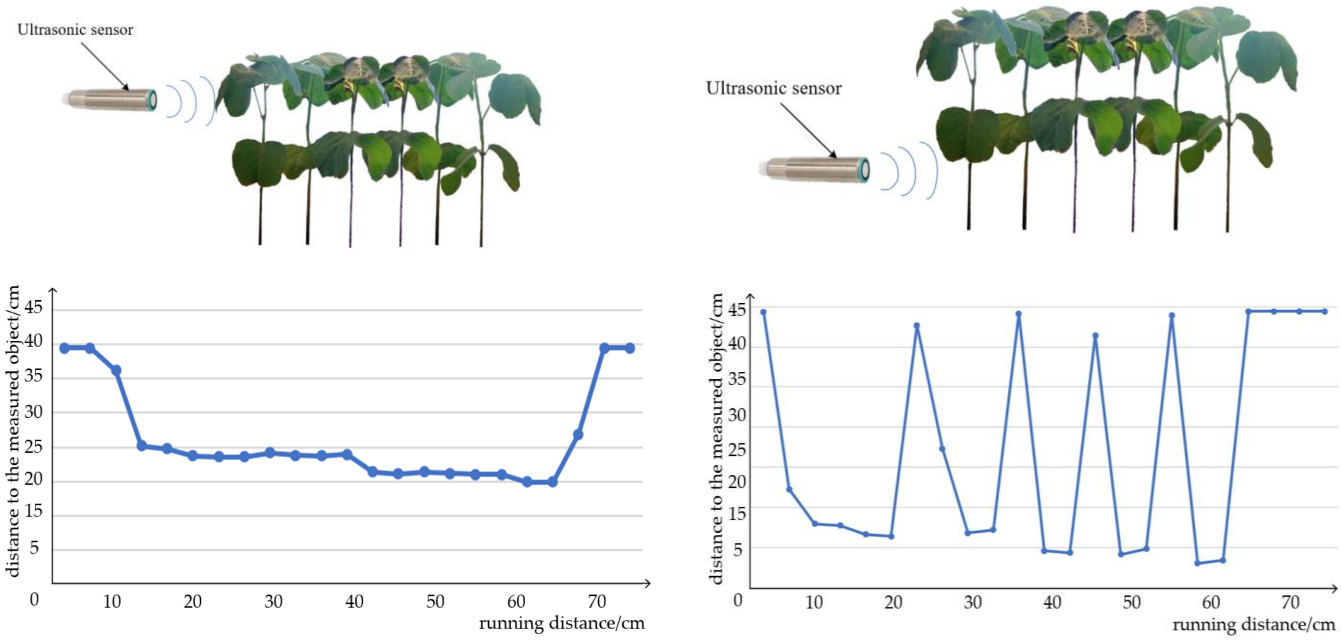

(**a**) (**b**)

Figure 16. Ultrasonic sensor detection object distance data graph: (**a**) ultrasonic sensor detection of the middle and upper parts of soybean plants; (**b**) ultrasonic sensor detection of the middle and lower parts of soybean plants.

In conclusion, the ultrasonic sensor is easily affected by the distance between the object to be measured, and the diameter of the object cannot be judged from the derived data. Therefore, ultrasonic sensors do not apply to the soybean recognition model in this paper.

The laser ranging sensor was then tested by placing the soybean plant on a conveyor belt and allowing the belt to run at a speed of 0.3 m/s. The laser range sensor was placed perpendicular to the conveyor belt and, in terms of height, was placed in the middle and lower portion of the soybean plant. When the laser ranging sensor detected the soybean plant passing by, the distance data was transmitted to the PLC via an analog current. A graph of the distance data derived from the PLC is shown in Figure 17, where the horizontal axis of the coordinates runs the distance. The vertical axis represents the distance between the sensor and the object under test.

Tests were perfomed to discern whether or not the laser range sensor can stably detect objects at different speeds and to discern whether of not laser range sensors would be affected by the distance between the objects to be measured. It was found that the sensor could accurately identify the number of objects to be measured, but still could not judge the diameter of the object to be measured from the image. After troubleshooting, it was found that the MicroWIN SMART software (V2.7) analog input, which comes with filter processing, had the acquisition frequency set to only 50 Hz. The parameters were then set to no filter processing input and an acquisition frequency of 400 Hz. Then, objects with diameters of 10 mm, 8 mm, 5 mm, and 3 mm were tested. As shown in Figure 18, the distance data plots for four different objects at a running speed of 0.2 m/s are shown.

An image of the distance data after processing by the algorithm is shown in Figure 19, and the diameters of different objects can be intuitively distinguished from the number of points in Figure 19.

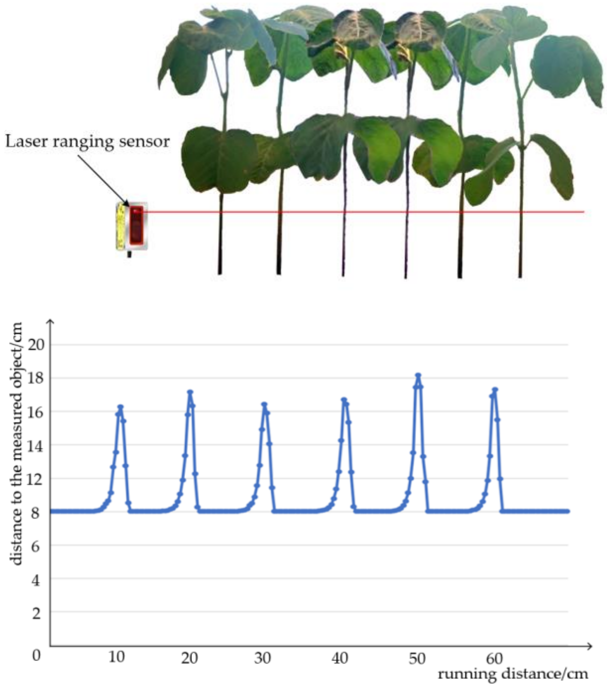

Figure 17. Laser ranging sensor detection object distance data graph.

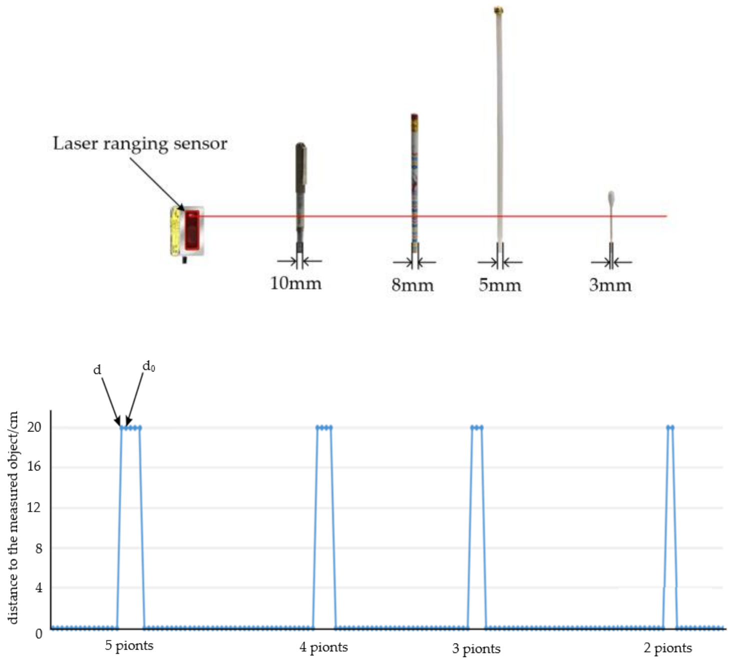

Figure 18. Distance data graph of objects with different diameters.

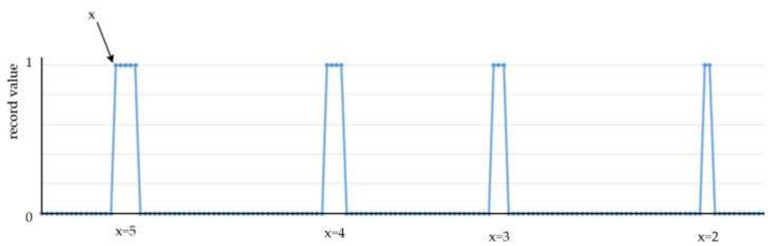

Figure 19. Distance data graph of objects with different diameters after algorithm processing.

The tests were run at 0.2 m/s, 0.3 m/s, 0.4 m/s, and 0.5 m/s, and the tests were repeated for three groups and summarized as shown in Table 3, where the "compare" is based on the number of points that should be required for the calculation.

Table 3. Table of the relationship between the diameter and number of points of the measured object at different speeds.

Speed/m·s^{-1}	Test Number	3 mm	5 mm	8 mm	10 mm
0.2	1	1	3	4	5
	2	2	3	4	5
	3	2	3	4	5
	compare	2	3	4	5
0.3	1	1	2	3	3
	2	1	2	3	3
	3	2	2	3	3
	compare	1	2	3	4
0.4	1	1	2	2	3
	2	1	2	2	2
	3	1	2	3	2
	compare	1	2	2	3
0.5	1	1	2	2	2
	2	1	1	3	2
	3	1	1	2	2
	compare	1	1	2	2

By analyzing the results of different object diameter detection tests, it was determined that the number of points can reflect the diameter of the object to be measured, and the speed of the running speed affects the number of points.

3.2. Experimental Process

The purpose of the test was mainly to verify the recognition rate of the soybean plant recognition model. As shown in Figure 20, there were 30 soybean plants at the trefoil stage, with an average height of about 250 mm and an average diameter of about 4 mm, from which, eight plants were randomly selected for the repetitive test. The tests were conducted in groups on a conveyor belt at speeds of 0.1 m/s, 0.2 m/s, 0.3 m/s, and 0.4 m/s. To verify the accuracy of the soybean plant identification model, in addition to detecting the conditions that satisfy the soybean plant identification model, the identification rates that satisfy the height-only condition, the diameter-only condition, and the height condition and diameter condition at the same time were further examined, and the tests in each group were replicated 20 times.

(**a**) (**b**)

Figure 20. Soybean plant: (**a**) thirty soybean plants; (**b**) eight randomly selected soybean plants.

When the laser range sensor does not detect a soybean plant, the mimicking elastic comb teeth of the weeding mechanism are in a closed state. As shown in Figure 21, a state diagram of the comb plate unfolding and closing is shown.

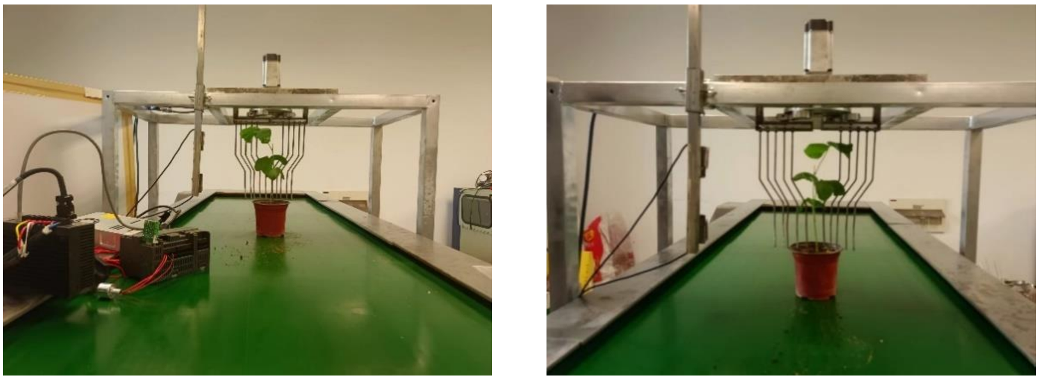

(a) (b)

Figure 21. Soybean plant position concerning elastic comb status: (**a**) elastic comb closure diagram; (**b**) elastic comb opening diagram.

Test process: as shown in Figure 22, the soybean plant moves forward with the conveyor movement, and then the laser ranging sensor detects the plant when the PLC distinguishes the soybean plant through the soybean recognition model. Next, the soybean plant passes through the weeding mechanism, and the PLC synchronizes to make the comb plate of the weeding mechanism unfold to allow the soybean plant to pass through smoothly. Finally, the comb plate is re-closed after the soybean plant passes through the weeding mechanism.

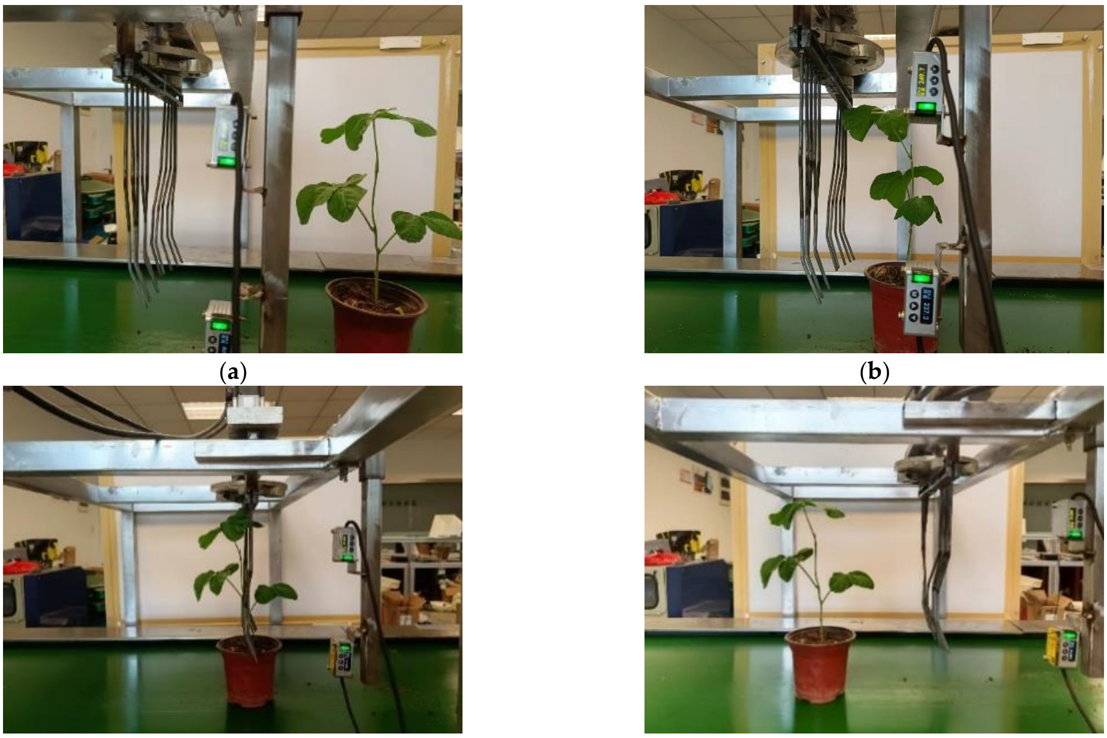

(a) (b) (c) (d)

Figure 22. Soybean plant position concerning elastic comb and sensor status during operation: (**a**) soybean plant not passing through elastic combs and sensors; (**b**) soybean plants detected by sensors; (**c**) elastic combs for seedling avoidance in soybean plant; (**d**) soybean plant passing through elastic combs and sensors.

3.3. Data Results and Analysis

During the test, manual counting was performed to count the number of soybean plants that successfully passed through the weeding mechanism after each set of tests.

As shown in Table 4, the results of the trials that only satisfied the height condition, only satisfied the diameter condition, and satisfied both the height condition and the diameter condition are shown. It was analyzed that when only the height condition was met, the recognition rate performed better at different speeds. Still, it was impossible to distinguish taller weeds from soybean plants by the height condition alone, so it was only used as a reference. When only the diameter condition was satisfied, the conveyor belt performed better when it operated at speeds up to 0.3 m/s. The diameter condition in the soybean plant identification model shows that when the object diameter is around 4 mm, a speed of 0.3 m/s or lower would result in a recorded value greater than or equal to 2, thus distinguishing soybean plants from weeds in terms of diameter. However, when the speed reaches 0.4 m/s, the recorded value will be greater than or equal to 1, and then the soybean plants and weeds cannot be well distinguished from each other in terms of diameter. The difference between the test results that satisfy both the height and diameter conditions and the test results that only satisfy the diameter conditions is small. The spacing condition should be added to carry out the soybean plant recognition model test to observe whether the soybean plant recognition model can better distinguish between soybean plants and weeds.

Table 4. Statistical table of soybean plant recognition rate.

Speed/m·s^{-1}	Height		Diameter		Height and Diameter	
	Amount	Recognition Rate	Amount	Recognition Rate	Amount	Recognition Rate
0.1	160	100%	160	100%	160	100%
0.2	160	100%	156	97.5%	158	98.75%
0.3	160	100%	140	87.5%	140	87.5%
0.4	148	92.5%	30	18.75%	32	20%

The experimental results of the soybean plant recognition model for detecting soybean plants are shown in Table 5. Because the recognition rate of 0.1 m/s can reach 100% for both height and diameter, and the actual detection of the running speed is too slow, this speed was no longer tested. Among the models, the soybean recognition model before optimization indicates that in the diameter condition, the recorded value of the diameter of the lower sensor is greater than or equal to 2. Since the soybean recognition model before optimization cannot distinguish well between soybean plants with a diameter of about 4 mm, the diameter condition is optimized. After the research found that the weeds around the soybean plants in the three-leaf stage are short, and that the individual taller weeds located in between the soybean plants can be excluded by using the spacing condition, the optimized soybean model should consider that when the diameter condition recorded value is greater than or equal to 1, the height and spacing conditions need to meet the requirements.

Table 5. Statistical table of recognition rate of soybean plant optimization recognition model.

Speed/m·s^{-1}	Before Optimizing the Soybean Recognition Model		After Optimizing the Soybean Recognition Model	
	Amount	Recognition Rate	Amount	Recognition Rate
0.2	160	100%	160	100%
0.3	142	88.75%	158	98.75%
0.4	36	22.5%	150	93.75%

Respectively, at running speeds of 0.2 m/s, 0.3 m/s, and 0.4 m/s, one set of distance data is exported for each. The distance data plots for each exported set are shown in Figure 23. Figure 24 is obtained after processing the data of the lower sensor, from which it is seen that at a speed of 0.2 m/s, the number of points at which the lower sensor detects the plant is greater than or equal to 2. The upper sensor detects the object, and the PLC determines the target object to be a soybean plant employing the pre-optimization soybean plant recognition model. At a speed of 0.3 m/s, individual plants are detected by the laser range sensor below with a point count of 1. Currently, the optimized soybean recognition model can determine the target object as a soybean plant. At a speed of 0.4 m/s, since the diameter of the soybean plant is around 4 mm, the diameter condition can no longer distinguish the soybean plant well. Hence, it is necessary to determine the target object as a soybean plant by the optimized soybean recognition model.

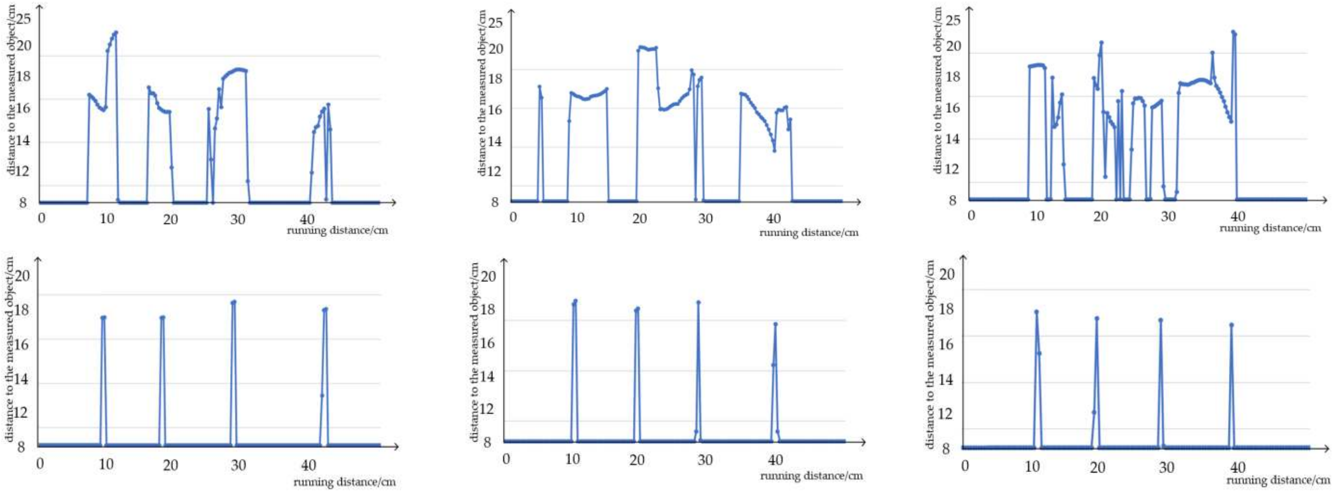

(**a**) (**b**) (**c**)

Figure 23. The plot of raw data from laser range sensors at different speeds: (**a**) 0.2 m·s^{-1} up and down laser ranging sensor raw data distance; (**b**) 0.3 m·s^{-1} up and down laser ranging sensor raw data distance; (**c**) 0.4 m·s^{-1} up and down laser ranging sensor raw data distance.

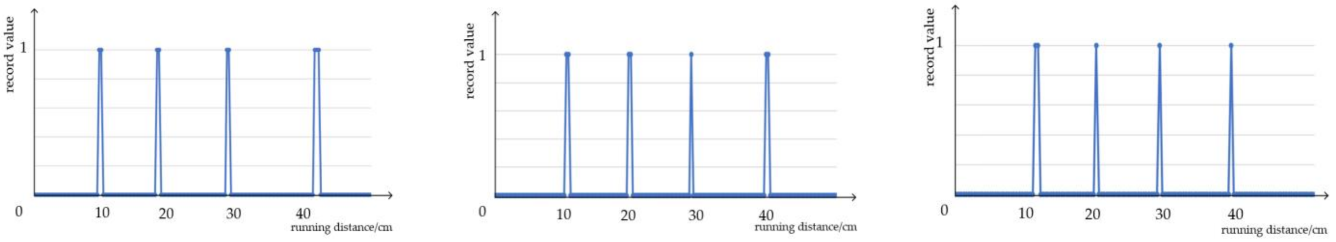

(**a**) (**b**) (**c**)

Figure 24. The plot of distance data processed by the laser rangefinder sensor algorithm below: (**a**) distance data processed by the sensor algorithm at a speed of 0.2 m·s^{-1}; (**b**) distance data processed by the sensor algorithm at a speed of 0.3 m·s^{-1}; (**c**) distance data processed by the sensor algorithm at a speed of 0.4 m·s^{-1}.

4. Discussion

Based on the observation of experimental results and analysis of data, it can be inferred that the soybean plant recognition model shows an improved recognition rate at a running speed of 0.2 m/s when incorporating the diameter condition, height condition, and spacing condition. Specifically, the recognition rate for the height condition is 100% at this speed. The optimized soybean recognition model, which includes the spacing condition in addition to the height condition, also achieves a recognition rate of 100%. At a running speed of

0.3 m/s, the improvement in the recognition rate of the soybean recognition model with the addition of the spacing condition is relatively small. However, the optimized soybean recognition model exhibits a significant increase in recognition rate and can effectively distinguish soybean plants. When the speed reaches 0.4 m/s, the unoptimized soybean recognition model has a lower recognition rate. Nevertheless, due to the generally shorter stature of weeds surrounding soybean plants in the three-leaf stage, even taller weeds between the plants can be filtered out using the spacing condition. At this speed, the optimized soybean recognition model can successfully differentiate soybean plants.

Taking comprehensive factors into consideration, the average diameter of soybean plants is around 4 mm. At a running speed of 0.4 m/s, according to Table 3, it can be inferred that there is a higher probability of having only one point detected under the diameter condition. Although the soybean plant recognition model can effectively distinguish soybean plants, there is still a certain probability of overlooking them. Additionally, according to the requirements of soybean agricultural cultivation, the distance between soybean plants should be 100 mm. If the running speed is too fast, the seedling damage rate of the weeding mechanism will increase. Therefore, at a speed of 0.3 m/s, the soybean recognition model can successfully differentiate soybean plants and the weeding mechanism can smoothly perform seedling avoidance actions. The experiments have shown that the soybean plant recognition model based on laser ranging sensors can effectively distinguish soybean plants, providing assistance to the mechanical weeding mechanism in performing successful seedling avoidance actions.

Image recognition has advantages for accurately identifying plants and weeds, as well as strong adaptability. However, image recognition is sensitive to environmental conditions such as lighting and shadows. The accuracy of recognition is often influenced by the complexity of the image background, the similarity between crops and weeds in morphology, and environmental factors. Laser radar recognition offers all-weather capability and high precision. However, it requires higher data processing and imposes higher demands on field environments. Image recognition requires the capturing of images of soybean plants using cameras, which are typically positioned above the plants. Laser radar, on the other hand, requires prior data collection of the scene within a certain range and is usually mounted on a mobile platform. In comparison, the laser ranging sensor used in this study is located between the intra-rows of soybean plants. Due to the different positions of image recognition devices and laser radar from the data acquisition device in this paper, other aspects of comparison are not applicable to this study.

Considering the complexity of the field environment, if the cotyledon position of soybeans is too low, typically, the width of the leaves exceeds the stem diameter. In this case, the lower laser sensor detects the leaves, while the upper laser sensor detects the plant. As a result, there will be a deviation in the positioning of the soybean plants, preventing the weeding mechanism from synchronously completing the seedling avoidance action accurately. Recognizing this limitation, further research and resolution will be conducted in future experiments.

5. Conclusions

1. Constructing a soybean plant recognition model, the problem of recognizing soybean plants and weeds was solved by the conditions of diameter, height, and soybean planting spacing of weeds.
2. The laser ranging sensor has the characteristics of high accuracy, high speed, and high stability. Compared with image recognition, it can avoid the influence of light, shadow, and other environmental factors and has a lower cost, so it is more effective. In the test process, the laser ranging sensor could be synchronized with the mechanical weeding device to achieve real-time detection, real-time weeding, and fast response without collecting data, and could then carry out weeding operations.
3. In the indoor test, the soybean plant recognition model programmed by PLC software had a recognition rate of 100%, 98.75%, and 93.75% at running speeds of 0.2 m/s,

0.3 m/s, and 0.4 m/s, respectively. Among them, the recognition rate of the soybean plant recognition model at the speed of 0.4 m/s could reach 93.75%. Still, it could not distinguish between soybean plants and weeds well according to the diameter conditions. There was a certain misjudgment for weeds with greater height, and the spacing between soybean plants was small, so it was not able to complete the role of weed control well at this speed. At the speed of 0.2 m/s, although the recognition rate could reach 100%, the running speed is slower, and the weeding efficiency is reduced. Our comprehensive analysis determined that the soybean plant recognition model performs better at the speed of 0.3 m/s, and the accuracy rate of soybean was as high as 98.75%. The test further verified the reliability and effectiveness of the method for distinguishing between soybean plants and weeds. The research results can provide a reference for recognizing soybean plants based on laser ranging sensors.

Author Contributions: Conceptualization, S.Y. and Y.J.; methodology, S.Y., X.X., Y.J. and Z.S.; software, S.Y. and Z.S.; validation, S.Y. and J.Y.; formal analysis, S.Y., Y.J. and Z.S.; investigation, S.Y. and J.Y.; resources, X.X., Y.J. and T.S.; data curation, S.Y. and Y.J.; writing—original draft preparation, S.Y.; writing—review and editing, S.Y. and Y.X.; visualization, S.Y. and Z.S.; supervision, X.X. and Y.J.; project administration, X.X. and Y.J.; funding acquisition, X.X. and Y.J. All authors have read and agreed to the published version of the manuscript.

Funding: This work was financially supported by the National Key R&D Program of China (No. 2022YFD2000700); Jiangsu Provincial Department of Agriculture and Rural Affairs (No. NJ2022-01); Innovation Program of Chinese Academy of Agricultural Sciences (No. CAAS-SAE-202301).

Institutional Review Board Statement: Not applicable.

Informed Consent Statement: Not applicable.

Data Availability Statement: The data presented in this study are available in the article.

Conflicts of Interest: The authors declare no conflict of interest.

References

1. Christopher, A.; Aaron, G.; Martin, M. Deteriorating weed control and variable weather portends greater soybean yield losses in the future. *Sci. Total Environ.* **2022**, *830*, 154764.
2. Wang, J.; Wang, W.; Ju, J.; Chen, X.; Wang, J.; Wang, H. Design and Test of Weeder between Rows in Rice Field Based on Remote Control Steering. *Trans. CSAM* **2021**, *52*, 97–105.
3. Xing, Q.; Ding, X.; Xue, X.; Cui, L.; Le, F.; Li, Y. Research on the development status of intelligent field weeding robot. *J. Chin. Agric. Mech.* **2022**, *43*, 173–181.
4. Fu, L.; Li, S.; Zhang, L.; Meng, Y. Research Progress on Field Weeding Robots: A Review. *Robot* **2021**, *43*, 751–768.
5. Wang, C.; Wu, X.; Zhang, Y.; Wang, W. Recognition and segmentation of maize seedlings in field based on dual attention semantic segmentation network. *Trans. Chin. Soc. Agric. Eng.* **2021**, *37*, 211–221.
6. Pérez-Ruiz, M.; Slaughter, D.; Gliever, C.; Upadhyaya, S. Automatic GPS-based intra-row weed knife control system for transplanted row crops. *Comput. Electron. Agric.* **2012**, *80*, 41–49. [CrossRef]
7. Cordill, C.; Grift, T. Design and testing of an intra-row mechanical weeding machine for corn. *Biosyst. Eng.* **2011**, *110*, 247–252. [CrossRef]
8. Ding, Y.; Zhan, P.; Zhou, Y.; Yang, J.; Zhang, W.; Zhu, K. Design and experiment of motion controller for information collection platform in field with Beidou positioning. *Trans. Chin. Soc. Agric. Eng.* **2017**, *33*, 178–185.
9. Zhang, J.; Gong, J.; Zhang, Y.; Mostafa, K.; Yuan, G. Weed Identification in Maize Fields Based on Improved Swin-Unet. *Agronomy* **2023**, *13*, 1846. [CrossRef]
10. Yang, S.; Zhang, H.; Xing, L.; Du, Y. Light weight recognition of weeds in the field based on improved MobileViT network. *Trans. Chin. Soc. Agric. Eng.* **2023**, *39*, 152–160.
11. Lin, C.; Hu, F.; Peng, J.; Wang, J.; Zhai, R. Segmentation and Stratification Methods of Field Maize Terrestrial LiDAR Point Cloud. *Agriculture* **2022**, *12*, 1450. [CrossRef]
12. Zhou, H.; Jin, S.; Zhou, L.; Guo, Z.; Sun, M. Recognition of camellia oleifera fruits in natural environment using multi-modal images. *Trans. Chin. Soc. Agric. Eng.* **2023**, *39*, 175–182.
13. Zhong, Y.; Huang, B.; Tang, C. Classification of Cassava Leaf Disease Based on a Non-Balanced Dataset Using Transformer-Embedded ResNet. *Agriculture* **2022**, *12*, 1360. [CrossRef]
14. Hu, L.; Luo, X.; Zeng, S.; Zhang, Z.; Chen, X.; Lin, C. Plant recognition and localization for intra-row mechanical weeding device based on machine vision. *Trans. Chin. Soc. Agric. Eng.* **2013**, *29*, 12–18.

15. Quan, L.; Zhang, J.; Jiang, W.; Li, H.; Yang, C.; Zhang, X. Development and Experiment of Intra-row Weeding Robot System Based on Protection of Maize Root System. *Trans. CSAM* **2021**, *52*, 115–123.
16. Liu, Y. Between Strains Weeding Machine Design, Simulation and Experimental Research. Master's Thesis, Henan Agricultural University, Zhengzhou, China, 2017.
17. Wu, W.; Tang, T.; Liu, Q.; Zhao, X.; Han, C.; Li, J. Semantic segmentation based road recognition technology of hilly fruit and tea garden. *J. Huazhong Agric. Univ.* **2022**, *41*, 246–254.
18. Shen, H.; Zhang, J.; Liu, D.; Ma, Q.; Zheng, G.; Zang, H. Wheat Seedling Counting Method with Enhanced Local Contextual Supervised Information. *Trans. CSAM* **2023**, *54*, 243–251.
19. Lan, Y.; Yan, Y.; Wang, B.; Song, C.; Wang, G. Current status and future development of the key technologies for intelligent pesticide spraying robots. *Trans. Chin. Soc. Agric. Eng.* **2022**, *38*, 30–40.
20. Reiser, D.; Vázquez-Arellano, M.; Paraforos, D.; Garrido-Izard, M.; Griepentrog, H. Iterative individual plant clustering in maize with assembled 2D LiDAR data. *Comput. Ind.* **2018**, *99*, 42–52. [CrossRef]
21. Jia, H.; Li, S.; Wang, G.; Liu, H. Design and experiment of seedling avoidable weeding control device for intertillage maize (*Zea Mays* L.). *Trans. Chin. Soc. Agric. Eng.* **2018**, *34*, 15–22.
22. Wang, J.; Yang, H.; Chen, Y.; Zhou, X.; Jiang, Y.; Zhang, J. Application analysis of domestic copying technology in agricultural machinery. *J. Chin. Agric. Mech.* **2023**, *44*, 31–39.
23. Chen, X.; Huang, Z.; Ma, X.; Qi, L.; Fang, G. Design and Experiment of Tactile Sensing Device for Measuring Rice Curvature. *Trans. CSAM* **2020**, *51*, 45–53.
24. Matteo, C.; Sara, F.; Paolo, S.; Sergio, M. Adaptive Ultrasound-Based Tractor Localization for Semi-Autonomous Vineyard Operations. *Agronomy* **2021**, *11*, 287.
25. Van der Linden, S.; Mouazen, A.; Anthonis, J.; Ramon, H.; Saeys, W. Infrared laser sensor for depth measurement to improve depth control in intra-row mechanical weeding. *Biosyst. Eng.* **2008**, *100*, 309–320. [CrossRef]